Neuroscience 130 (2005) 911–925

HEMISPHERIC ASYMMETRY, MODULAR VARIABILITY AND AGE-RELATED CHANGES IN THE HUMAN ENTORHINAL CORTEX

G. SIMIC,[a]* S. BEXHETI,[a] Z. KELOVIC,[a] M. KOS,[b] K. GRBIC,[a] P. R. HOF[c] AND I. KOSTOVIC[a]

[a]*Department of Neuroscience, Croatian Institute for Brain Research, Zagreb University Medical School, Salata 12, Zagreb 10000, Croatia*

[b]*Department of Pathology, University Hospital "Sisters of Mercy," Vinogradska 29, Zagreb 10000, Croatia*

[c]*Departments of Neuroscience, Geriatrics and Adult Development, and Ophthalmology, Mount Sinai School of Medicine, New York, NY 10029, USA*

Abstract—The verrucae areae entorhinalis (VAE) are a characteristic feature of the human brain that occupy the anterior and posterolateral parts of the parahippocampal gyri and correspond to the islands of layer II neurons. We analyzed VAE in 60 neurologically normal subjects ranging from 23 to 85 years of age using a casting method. In 10 of these subjects the total number of neurons in the entorhinal islands was estimated stereologically using the optical fractionator. The number and surface area of VAE were higher in the left hemisphere compared with the right, and this leftward asymmetry was highly significant. Regression analysis showed a negative correlation between average VAE area and age in both hemispheres, representing a rate loss of about 800 μm^2 per year. The estimated number of neurons obtained with the optical fractionator showed no significant difference between the left and the right hemisphere (468,000±144,000 vs. 405,000±117,000). There was a highly significant negative correlation between neuron numbers and age in both sides. In addition, clusters of small, undifferentiated layer II neurons ('heterotopias') were frequently observed in the rostral part of the entorhinal cortex in young and elderly adults.

Layer II entorhinal neurons are among the first to show neurofibrillary changes during normal aging. The present data confirm the occurrence of age-related neuron loss in the entorhinal cortex. Considering the consistent projections from ipsilateral auditory association areas that, together with Broca's motor-speech area (Brodmann areas 44 and 45), show leftward asymmetry from early infancy (such as Brodmann area 22, planum temporale, and area 52 in the long insular gyrus), we speculate that functional lateralization of the human entorhinal cortex may be associated with specialization for memory processing related to language. Due to the dependence of hippocampal formation on entorhinal projections, this finding is also consistent with the greater capacity of the left hippocampus for verbal episodic memory.

Key words: aging, Alzheimer's disease, cerebral dominance, hippocampus, language, schizophrenia.

*Corresponding author. Tel: +385-1-459-6807; fax: +385-1-459-6942.
E-mail address: gsimic@hiim.hr (G. Simic).

Abbreviations: AD, Alzheimer's disease; asf, area sampling fraction; ssf, section sampling fraction; tsf, fraction of the section thickness sampled; VAE, verrucae areae entorhinalis.

Asymmetries in the size of brain regions have been associated with functional lateralization. Since Broca's discovery of the left hemisphere dominance for language abilities (Broca, 1861, 1865), many structural and functional asymmetries have been reported in the human brain, as well as in non-human primates (Gannon et al., 1998; Sherwood et al., 2003). The cortical structures of the human brain with documented anatomical asymmetries (left commonly larger than right) include the anterior speech region (pars opercularis and pars triangularis of the gyrus frontalis inferior; Falzi et al., 1982; Amunts et al., 1999, 2003), association auditory cortex (planum temporale; Pfeifer, 1936; Geschwind and Levitsky, 1968), and area PG in the inferior parietal lobule (Eidelberg and Galaburda, 1984). The existence of an asymmetry probably related to language function has also been shown in some subcortical structures, such as the lateral posterior nucleus of the thalamus (Eidelberg and Galaburda, 1982) and the subputaminal nucleus (Simic et al., 1999).

A functional asymmetry of the entorhinal cortex with the left (dominant) being more involved in verbal and the right in non-verbal processing has been proposed (Tranel, 1991; Eustache et al., 2001). However, whether functional asymmetry of the entorhinal cortex is accompanied by structural asymmetry, such that more neurons and possibly their connections are formed within the left hemisphere, is unclear. With the exception of sulcal patterns (Heinsen et al., 1996; Hanke, 1997), only one study has investigated other possible anatomic and cytoarchitectonic left-right asymmetries in the human entorhinal cortex (Heinsen et al., 1994).

The entorhinal region in the human brain spreads over the gyrus ambiens and a considerable part of the parahippocampal gyrus (Brodmann, 1909; Braak, 1972). Small elevations with shallow grooves in between are present on the surface of these gyri. Retzius first observed these elevations and to describe them coined the term "verrucae gyri hippocampi" (Retzius, 1896). Ramón y Cajal (1901–1902), von Economo (1927) and von Economo and Koskinas (1925) showed that they are formed from groups ('glomeruli') of layer II neurons which cause an elevation on the cortical surface. These verrucae are a unique feature that define the entorhinal region macroscopically in humans, and allow for its delineation even with the unaided eye (Klingler, 1948; Braak, 1980; Braak and Braak, 1992; Heinsen et al., 1994; Insausti et al., 1995; Solodkin and Van Hoesen, 1996). We designate them thereafter as the verrucae areae entorhinalis (VAE).

During the course of normal aging and in Alzheimer's disease (AD), layer II neurons of the entorhinal cortex are among the first to show neurofibrillary changes, and probably

0306-4522/05$30.00+0.00 © 2004 IBRO. Published by Elsevier Ltd. All rights reserved.
doi:10.1016/j.neuroscience.2004.09.040

Table 1. Case information and data from VAE analysis

Case no.	Gender	Age (yr.)	Number of VAE in left EC[a]	Number of VAE in right EC	Total area of VAE in left EC (mm^2)	Total area of VAE in right EC (mm^2)	Average area of single left VAE (mm^2)	Average area of single right VAE (mm^2)	Asymmetry coefficient (δ)	Cause of death
1	F	23	99	81	31	27	0.313	0.333	−0.138	Traffic accident
2	F	25	110	95	35	32	0.318	0.337	−0.090	Traffic accident
3	F	25	105	89	34	32	0.324	0.360	−0.061	Homicide
4	M	26	109	102	32	31	0.294	0.304	−0.032	Traffic accident
5	M	27	106	81	34	31	0.321	0.382	−0.092	Traffic accident
6	M	27	110	90	35	33	0.318	0.367	−0.059	Freezing
7	M	27	115	110	34	31	0.296	0.282	−0.092	Traffic accident
8	F	27	117	107	35	31	0.299	0.290	−0.121	Homicide
9	F	28	120	118	35	31	0.292	0.258	−0.121	Homicide
10	F	28	110	99	35	32	0.318	0.323	−0.090	Breast carcinoma
11	F	29	110	108	35	32	0.318	0.296	−0.090	Traffic accident
12	F	30	112	108	34	32	0.304	0.296	−0.061	Traffic accident
13	F	30	110	109	35	30	0.318	0.275	−0.154	Homicide
14	M	31	120	110	40	38	0.333	0.345	−0.051	Homicide
15	M	32	122	109	40	38	0.328	0.349	−0.051	Homicide
16	F	33	110	108	35	32	0.318	0.296	−0.090	Traffic accident
17	M	34	118	110	34	31	0.288	0.282	−0.092	Traffic accident
18	F	36	120	119	34	32	0.283	0.269	−0.061	Traffic accident
19	M	36	121	118	33	31	0.273	0.263	−0.094	Traumatic shock
20	F	36	111	89	30	27	0.270	0.303	−0.105	Traffic accident
21	F	39	125	118	30	28	0.240	0.237	−0.069	Traffic accident
22	M	40	115	109	32	30	0.278	0.275	−0.065	Peritonitis
23	M	40	110	102	31	30	0.282	0.294	−0.033	Cirrhosis
24	M	41	109	97	26	26	0.239	0.268	0.000	Traffic accident
25	F	41	120	109	37	32	0.308	0.294	−0.145	Homicide
26	M	41	98	75	31	29	0.316	0.387	−0.067	Myocardial infarction
27	F	42	111	102	30	29	0.270	0.284	−0.034	Homicide
28	M	43	120	115	37	32	0.308	0.278	−0.145	Traffic accident
29	M	43	122	112	39	33	0.320	0.295	−0.167	Homicide
30	F	43	123	113	32	31	0.260	0.274	−0.032	Cirrhosis
31	F	45	127	113	35	31	0.276	0.274	−0.121	Breast cancer
32	M	45	126	120	34	32	0.270	0.267	−0.061	Traffic accident
33	M	46	122	118	37	32	0.303	0.271	−0.145	Traffic accident
34	M	47	122	114	34	31	0.279	0.272	−0.092	Cirrhosis
35	M	48	137	122	39	37	0.285	0.303	−0.053	Myocardial infarction
36	M	49	120	117	39	37	0.325	0.316	−0.053	Traffic accident
37	M	50	125	120	28	26	0.224	0.217	−0.074	Myocardial infarction
38	M	50	130	115	32	30	0.246	0.261	−0.065	Homicide
39	M	51	104	97	31	30	0.298	0.309	−0.033	Lung cancer
40	M	51	118	99	32	30	0.271	0.303	−0.065	Myocardial infarction
41	F	53	125	122	34	33	0.272	0.270	−0.030	Colon cancer
42	M	54	133	123	40	33	0.301	0.268	−0.192	Homicide
43	M	55	129	111	35	32	0.271	0.288	−0.090	Traffic accident
44	F	55	119	109	34	33	0.286	0.303	−0.030	Myocardial infarction
45	F	57	115	110	34	32	0.296	0.291	−0.061	Colon cancer
46	M	58	130	125	32	30	0.246	0.240	−0.065	Cerebral infarction
47	F	59	125	119	30	29	0.240	0.244	−0.034	Traffic accident
48	F	59	123	113	32	32	0.260	0.283	0.000	Cirrhosis
49	M	64	142	132	41	36	0.289	0.273	−0.130	Colon cancer

Table 1. Continued

Case no.	Gender	Age (yr.)	Number of VAE in left EC[a]	Number of VAE in right EC	Total area of VAE in left EC (mm^2)	Total area of VAE in right EC (mm^2)	Average area of single left VAE (mm^2)	Average area of single right VAE (mm^2)	Asymmetry coefficient (δ)	Cause of death
50	M	65	127	119	35	32	0.276	0.269	−0.090	Cardiopulmonary insuff.
51	M	68	137	128	41	40	0.299	0.313	−0.025	Myocardial infarction
52	M	70	149	131	42	33	0.282	0.252	−0.240	Cardiopulmonary insuff.
53	M	71	119	110	35	32	0.294	0.291	−0.090	Myocardial infarction
54	F	73	156	136	40	38	0.256	0.279	−0.051	Cardiopulmonary insuff.
55	F	75	127	115	32	30	0.251	0.261	−0.065	Traffic accident
56	M	80	148	118	37	32	0.250	0.271	−0.145	Myocardial infarction
57	M	80	128	115	34	32	0.266	0.278	−0.061	Cerebral hemorrhage
58	M	80	130	125	39	33	0.300	0.264	−0.167	Subarachnoidal bleeding
59	M	83	139	127	38	34	0.273	0.268	−0.111	Colon cancer
60	F	85	141	128	39	32	0.277	0.250	−0.197	Traffic accident

[a] EC, entorhinal cortex.

are the first to die, resulting in smaller VAE which eventually disappear due to this cell loss (Hyman et al., 1986; Van Hoesen et al., 1991; Braak and Braak, 1991; Bouras et al., 1993, 1994; Gómez-Isla et al., 1996; Giannakopoulos et al., 1998; Simic et al., 2000; Hof et al., 2003). Many studies also point to entorhinal cortex abnormalities in schizophrenia. One of the most commonly reported is the poor development of clusters of layer II neurons (Jakob and Beckmann, 1986; Falkai et al., 1988; Arnold et al., 1991).

Following our initial observations (Bexheti et al., 1988; Kelovic et al., 1988), the goal of this study was to determine precisely the number and surface area of VAE as well as size, shape and total number of neurons in the entorhinal islands on a larger sample of human brains. The observations reported here provide a quantitative characterization of the extent and modular organization of the entorhinal cortex in human, reveal possible hemispheric and gender differences as well as possible changes during aging, and provide normative parameters for investigations of pathologic conditions affecting the entorhinal cortex.

EXPERIMENTAL PROCEDURES

The brains of 60 normal individuals, between the ages of 23 and 85 (25 women and 35 men) were obtained between 1976 and 1987 from the Departments of Forensic Medicine at the University Medical School Zagreb and the University Medical School Pristina during routine autopsies in accordance with the law and under the control of the Ethical Committee of the Zagreb Medical School. Only subjects with no neuropsychiatric illnesses and no neurologic evidence of vascular or neurodegenerative lesions based on their medical records, and for whom the postmortem interval did not exceed 24 h (mean 9.8±4.4 S.D.), were analyzed. Brains from subjects who died due to traffic accidents or brain trauma (such as no. 46, 57 and 58) were used only if there were no visible injuries to the temporal lobe. The age, gender and the cause of death of each subject are shown in Table 1. Unfortunately, we had only incidental reports on handedness, but no formal, detailed testing of the subjects. With respect to agonal state of subjects included in the study, the population studied was comparable to other published reports (Gómez-Isla et al., 1996, 1997; Simic et al., 1997; Hof et al., 2003). Since non-demented elderly subjects do not exhibit significant loss of neurons (Hof et al., 2003, among others), it would seem unlikely that the inter-individual differences in agonal state represented a serious confound for the obtained results on neuron numbers.

After extraction from the skull, the whole brains were fixed in 10% neutral formalin. The brains were suspended by the basilar artery during the fixation process. After a short primary fixation, the block of tissue comprising the uncus and parahippocampal gyrus was isolated and immersed in 10% fresh neutral formalin for up to 7 days. The meninges were carefully removed from the surface by using microsurgical instruments and a stereomicroscope.

In order to demonstrate the presence of VAE as precisely as possible we utilized a method for taking casts using silicone-based impression materials (Optosil/Xantopren; Heraeus Kulzer, Dormagen, Germany) used in dental prosthetics. To avoid artifacts, the surface of the specimen was quickly dried under a hot air stream prior to print taking. After the first mold made of Optosil had hardened, it was filled with Xantopren and then, using gentle pressure, the specimen was pressed into the mold. The specimen was not removed until the Xantopren had hardened. In such endocasts, all indentations that corresponded to the VAE were visible under a stereomicroscope. Each indentation was delineated using a thin black waterproof marker (Fig. 1A). Special attention was paid in cases where the entorhinal cortex extended into the opening and medial bank of the collateral fissure, because at these locations VAE were not reliably reflected on the casts. In such cases, after visual inspection, the specimens were embedded in paraffin, serially cut at 20 μm in the frontal plane, stained with Cresyl Violet and microscopically analyzed for total number of VAE. Planimetric analysis and graphic reconstruction of the surface area occupied by the VAE were made from the casts using a Robotron Reiss planimeter (Budapest, Hungary) and a

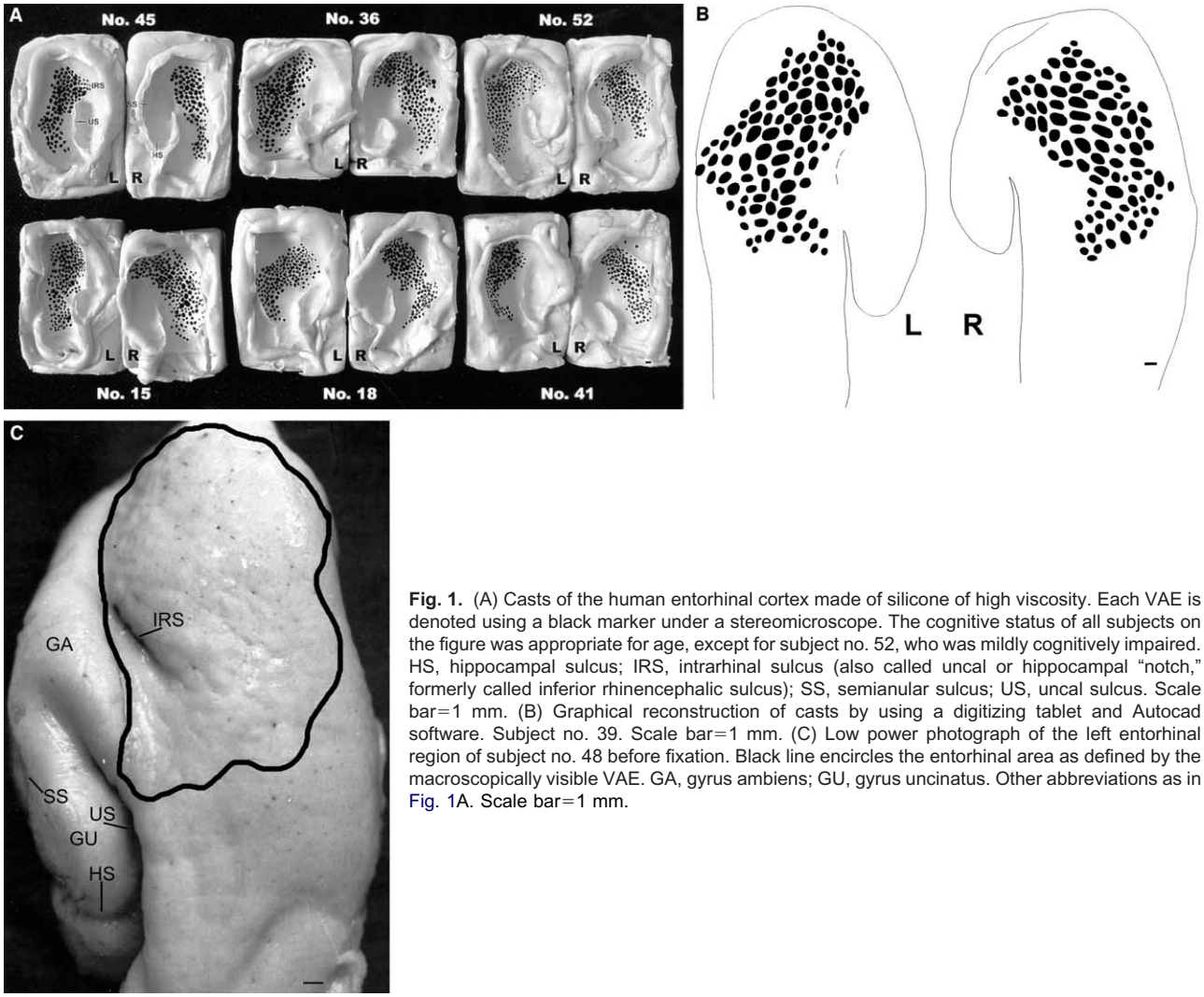

Fig. 1. (A) Casts of the human entorhinal cortex made of silicone of high viscosity. Each VAE is denoted using a black marker under a stereomicroscope. The cognitive status of all subjects on the figure was appropriate for age, except for subject no. 52, who was mildly cognitively impaired. HS, hippocampal sulcus; IRS, intrarhinal sulcus (also called uncal or hippocampal "notch," formerly called inferior rhinencephalic sulcus); SS, semianular sulcus; US, uncal sulcus. Scale bar=1 mm. (B) Graphical reconstruction of casts by using a digitizing tablet and Autocad software. Subject no. 39. Scale bar=1 mm. (C) Low power photograph of the left entorhinal region of subject no. 48 before fixation. Black line encircles the entorhinal area as defined by the macroscopically visible VAE. GA, gyrus ambiens; GU, gyrus uncinatus. Other abbreviations as in Fig. 1A. Scale bar=1 mm.

Genius graphic tablet GT1212A under the control of ACAD 10E software (Autodesk, San Rafael, CA, USA; Fig. 1B). For better orientation, a low power photograph of the entorhinal region as defined by the macroscopically visible VAE is shown in Fig. 1C. To correct for variability in brain size, for each subject an asymmetry coefficient (δ) was calculated using the formula: δ=(right entorhinal area−left entorhinal area)/0.5×(right entorhinal area+left entorhinal area) (Galaburda et al., 1987).

Thirteen (seven left and six right) out of the 120 hemispheric specimens were embedded in celloidin (Cedukol; Merck, Darmstadt, Germany) after casting, serially cut at 20 μm in the tangential plane, stained with Cresyl Violet and reconstructed using a calibrated projecting Visopan microscope (Reichert, Vienna, Austria; Fig. 2B). Layer II neurons defined as large, darkly stained, stellate, modified pyramidal and multipolar cells were easily distinguished from layer III medium-sized pyramidal neurons. The 23–33 tangential sections that contained all of the entorhinal islands were subjected to neuron counts using the fractionator method (West et al., 1991). A systematic–random sampling design was used to sample every sixth section that contained entorhinal islands (the section sampling fraction, ssf, was therefore 0.167; Gundersen, 1986; Simic et al., 1997). All layer II neurons were counted in disectors that were systematically positioned along the two axes of the section plane with a random start. This was accomplished using the meander algorithm function of the StereoInvestigator software and microscope-computer interface system (MicroBrightField, Williston, VT, USA), so that the microscope stage automatically moved to sampling positions that corresponded to a randomly placed rectangular lattice of points in the section plane. The distance between these positions along each axis was 980 μm (a_{step}=0.96×10^6 μm^2), while the area of the disector counting frame was 5256 μm^2 (i.e. the area sampling fraction, asf, was 0.05475). Since thickness of the sections was 20 μm and the thickness of the disector was 10 μm, the fraction of the section thickness sampled at each point, tsf, was 0.5. Optical disectors were used to count the number of neurons (Q^-) at each of the positions in the sampling grid, as described in detail previously (Simic et al., 1997; West and Slomianka, 1998). Finally, the total number of neurons (N), was estimated using the formula: $N=\Sigma\ Q^- \times(1/ssf)\times(1/asf)\times(1/tsf)$.

In addition, after the cryoprotection and sectioning, 80-μm-thick free-floating sections of rostral part of entorhinal cortex from three neurologically normal subjects aged 19, 32 and 57 years were processed for calbindin and parvalbumin immunohistochemistry using a Vectastain ABC kit (Vector Laboratories, Burlingame, CA, USA). Both primary monoclonal anti-calbindin-D28k and parvalbumin antibody (Sigma, St. Louis, MO, USA) were used at a dilution of 1:1000. For controls the primary antiserum was omitted.

The statistical analysis was carried out using the Statistica v5.0 program (Statsoft, Tulsa, OK, USA). The age-related changes in number and size of VAE, as well as for neuronal loss, were described with the Pearson's coefficient of correlation (r) and evaluated by testing the linear regression. Regressions with $2P$ values of Pearson's coefficient of correlation less than 5% were defined as statistically significant. Hemisphere- and gender-related differences in the number of VAE, area of VAE and asymmetry coefficient were evaluated with paired (two-sided) Student's t-test. A value of P less than 0.05 was chosen as the criteria for the level of confidence. Age-related changes in the number of VAE were tested using one-way analysis of variance (with age as a mean factor). Post hoc analysis between defined groups of subjects (20–29, 30–39, 40–49, 50–59, 60–69, 70–79 and 80–89 years of age) was done by using Scheffé's method.

RESULTS

Both the rhinal and collateral sulci were fully present in all of the investigated hemispheres. No macroscopically noticeable differences in the major sulcal patterns were observed between the right and left hemispheres, and between genders. In eight out of 120 hemispheres, the entorhinal cortex extended significantly into the medial bank of the collateral fissure so that VAE located in this part of entorhinal cortex could not reliably be imprinted on the casts. In these cases, the number of VAE was counted by visual inspection and subsequent histologic verification for layer II cell islands on coronally cut, Nissl-stained sections. As observed from the casts, the overall difference in the modular variability among the subjects was striking, no two casts being similar (Fig. 1A). Thus, the interindividual variability of entorhinal modules appears to be reflected in differences in size, number, and distribution of the islands, possibly creating 'individual entorhinal fingerprints.' The main characteristic of most VAE (particularly those located rostro-medially) was their elongated, ellipsoid shape, with the longer axis oriented in the rostrocaudal direction of the parahippocampal gyrus. As the axis of the parahippocampal gyrus rotates by about 180° at the anterior aspect of the uncus, the long axis of the VAE usually was aligned along this curvature. The width of individual entorhinal islands on histological sections usually varied from 0.25 to 0.8 mm and their length varied from 0.2 to 1.2 mm. The majority of VAE ranged in size from about 0.7×0.5 mm to 1.2×1 mm (longer axis×shorter axis dimensions). The largest VAE was 2.11×1.95 mm, and the smallest 0.53×0.48. The number of VAE, the total surface of VAE, the average area of single VAE, as well as the asymmetry index of all of the studied brains are shown in Table 1. As seen on tangential sections (Fig. 2), neighboring VAE were often connected by narrow bridges of cells. The distance between VAE was generally shorter laterally. A series of Nissl plates that demonstrate the most salient features of the entorhinal cortex on coronal sections is given in Fig. 2C–E.

Clusters of small, undifferentiated spindle-shaped or bipolar neurons were commonly found in the olfactory and lateral rostral subfields (according to the nomenclature of Insausti et al., 1995), independent of the age of subjects (Fig. 3A, B). Most of these neurons had the morphology of late neuroblasts or "immature" neurons (Rakic and Nowakowski, 1981), and were easily distinguished from the differentiated neurons of the entorhinal cortex. Because these cells may be small GABAergic interneurons, immunohistochemistry for the calcium-binding proteins calbindin and parvalbumin was performed. Very rare cells had faint calbindin immunoreactivity (Fig. 3C). Almost no positive parvalbumin labeling of these cells was observed (Fig. 3D), indicating that these ectopic cells are unlikely to represent a population of inhibitory interneurons.

Numbers of VAE

The mean total number of VAE of all the studied brains was 232 (range: 173–292, S.D.=23.9), and on average 116 per hemisphere (range: 75–156, S.D.=13.3). The mean number of VAE in the left hemisphere was 121 (range: 98–156, S.D.=12.0), while the mean number of VAE in the right hemisphere was 111 (range: 75–136, S.D.=12.7). The number of VAE was significantly higher in the left than in the right hemisphere (t=4.56, df=118, $P<0.001$; Fig. 4). The mean number of VAE was higher in the left hemisphere in both women (118.8±11.8 vs. 109.5±12.3, t=2.75, df=48, $P<0.01$) and men (123.1±12.0 vs. 112.2±13.1, t=3.66, df=68, $P<0.001$; Fig. 4). Men had slightly higher mean value of VAE in both left and right hemisphere, but this difference was not statistically significant (Fig. 4).

Area of VAE and asymmetry index

The mean total area of VAE in all of the studied brains was 66.4 mm^2 (range: 52.0–81.1 mm^2, S.D.=6.0 mm^2). The mean area of VAE for the left hemisphere was 34.7 mm^2 (range: 26.2–42.3 mm^2, S.D.=3.4 mm^2), while the mean VAE area in the right hemisphere was 31.8 mm^2 (range: 25.8–40.0 mm^2, S.D.=2.8 mm^2). The area of VAE was significantly higher in the left than the right hemisphere (t=5.11, df=118, $P<0.001$; Fig. 5). The mean area of VAE was larger in the left hemisphere in both women (33.9±2.6 mm^2>31.2±2.2 mm^2, t=2.75, df=48, $P<0.01$) and men (35.3±3.9 mm^2>32.2±3.1 mm^2, t=3.66, df=68, $P<0.001$; Fig. 5). Men had slightly higher mean value of VAE area in both hemispheres than women, but this difference did not reach statistical significance (Fig. 5). The mean value of the asymmetry coefficient δ was −0.086 (minimum −0.24, maximum 0.00, S.D.=0.049). A leftward asymmetry was highly significant (t=13.42, $P<0.001$). The difference in asymmetry between men and women was not statistically significant.

VAE and neuron number changes with aging

During aging, a trend toward an increase in the total number of VAE was observed, at a rate of approximately 1 VAE per year. The difference was significant among defined age groups (ANOVA, F=8.77, df=59, $P<0.01$). The post hoc analysis using Scheffé's method showed marked difference only when comparing subjects aged 20–29 years with groups of subjects aged 50–59 ($P<0.05$), 60–69 ($P<0.01$), 70–79 ($P<0.01$) and 80–89 ($P<0.001$) years of age. The equation of the linear regression line was: number of VAE=185.5+(age in years); Pearson's r=0.71). However, this trend was not reflected by a substantial increase of the total VAE area (VAE area=61.9+0.1×(age in years);

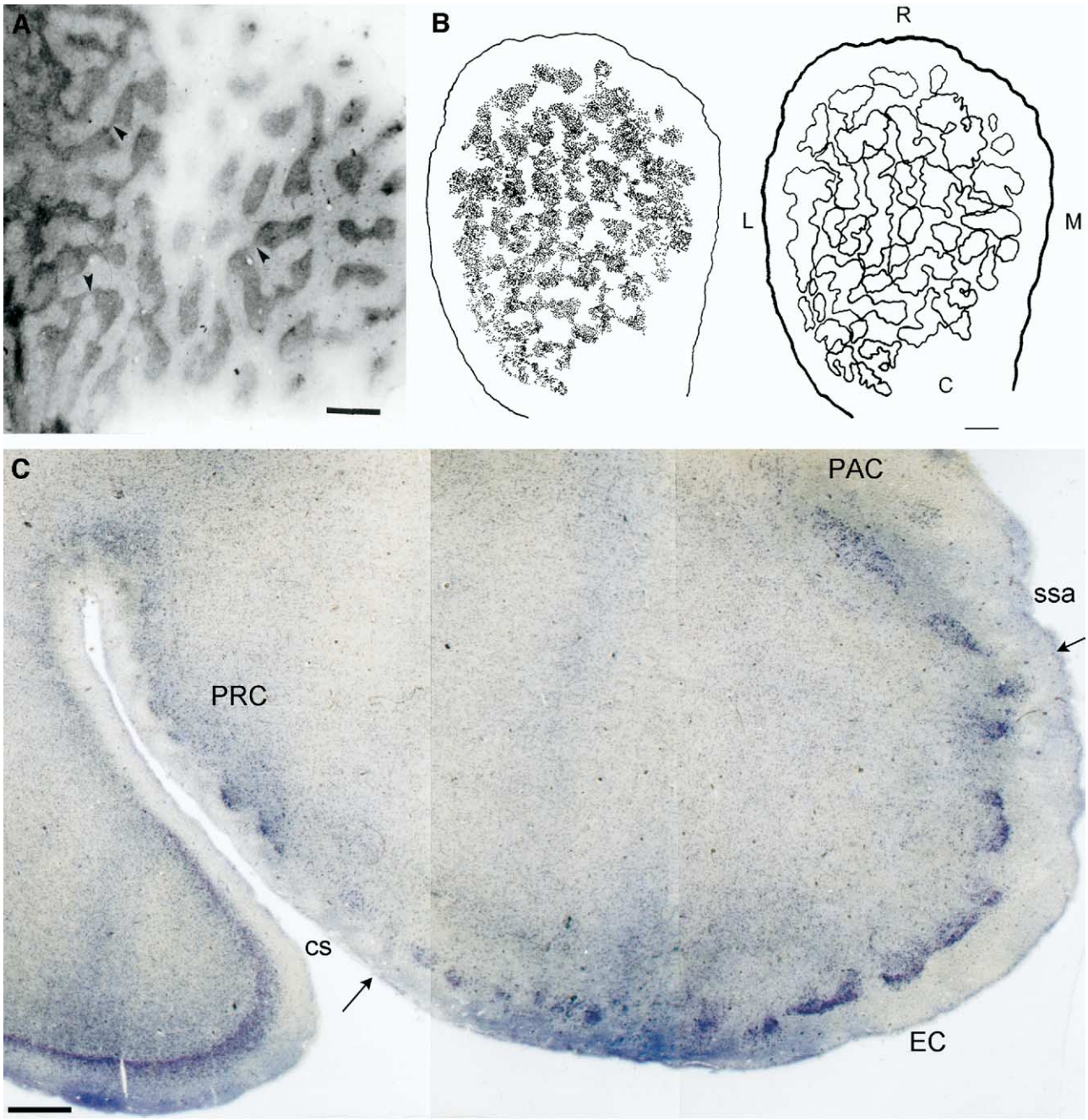

Fig. 2. (A) Illustration of entorhinal modules on a tangential section. Due to the convoluted shape of the entorhinal cortex and the section thickness, some of the islands of layer II entorhinal neurons are not visible. Note that islands may be connected with bridges of layer II neurons (arrowheads). Nissl stain. Subject no. 15, left hemisphere. Scale bar=1 mm. (B) Illustration of reconstruction of entorhinal cortex islands from tangential sections and their consequent delineation before fractionator analysis. C, caudal side; L, lateral; M, medial; R, rostral. Subject no. 59, left hemisphere. Scale bar=1 mm. (C–E) Delineation of entorhinal cortex on coronal sections (arrows). A, amygdala; C, rostral level; cs, collateral sulcus; D, intermediate level; E, caudal level; FD, fascia dentata; H, hippocampus; hf, hippocampal fissure; PAC, periamygdaloid cortex; PRC, perirhinal cortex; ssa, sulcus semianularis; U, uncus; V, ventricle. Scale bar=2 mm.

$r=0.27$). Regression lines showed negative correlations between average VAE area and age of similar magnitude in both hemispheres (Fig. 6). The mean VAE area in the left entorhinal cortex was calculated as $0.322-0.0007\times$(age in years) mm^2 ($r=-0.48$; Fig. 6), and $0.333-0.0009\times$(age in years) mm^2 ($r=-0.46$) in the right entorhinal cortex (Fig. 6). The average area of single VAE decreased similarly in both left and right entorhinal cortices ($r=-0.48$ for left, $r=-0.46$ for right hemisphere), representing a decrease rate of approximately 800 μm^2 per year.

Stereological estimates obtained using the optical fractionator showed that 468,000±144,000 neurons in ento-

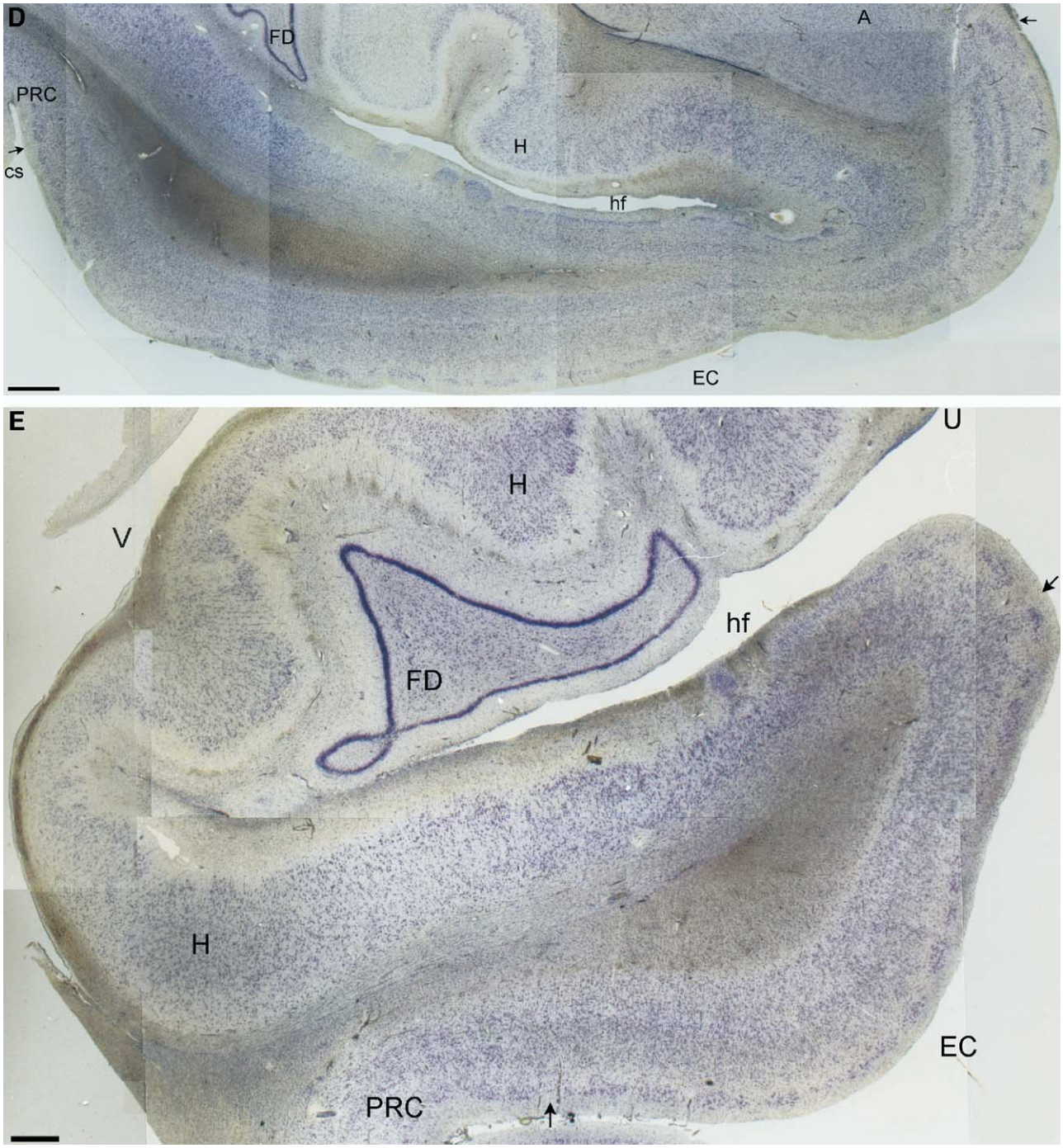

Fig. 2. (*Continued*).

rhinal islands in the left and 405,000±117,000 neurons in the right hemisphere were present (Table 2). There was no significant difference between left and right sides (t=0.9, df=11, P>0.05), while regression lines (Fig. 7) showed nearly a identical degree of neuron loss during aging (left: N_N=0.874−0.008×(age in years)×10^6; Pearson's r=−0.91, right: N_N=0.791−0.006×(age in years)×10^6; Pearson's r=−0.93; Table 3).

DISCUSSION

The present findings show that determination of the number and area of VAE on casts of the ambient and parahippocampal gyri, and area and number of neurons in entorhinal islands provide us with quantitative parameters about the modular organization of the entorhinal cortex in a large sample of human brains. The number and area of VAE are substantially

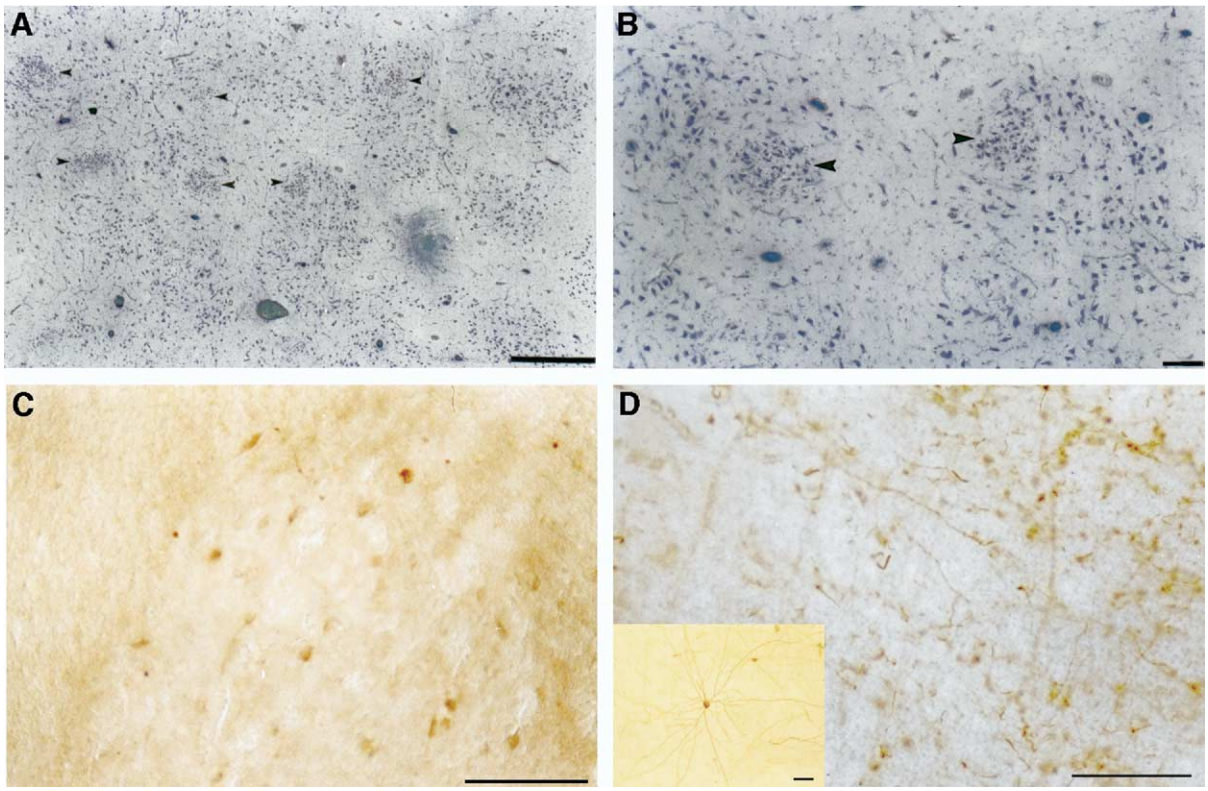

Fig. 3. (A) Clusters of small, undifferentiated ('immature') neurons in the rostral part of the entorhinal cortex in 70 year old brain (arrowheads). Subject no. 52, left hemisphere. Scale bar=500 μm. (B) Higher magnification of the central part of panel A. Calbindin (C) and parvalbumin (D) labeling of sections adjacent to A. Inset in figure D shows parvalbumin-immunoreactive neuron in the same section. Scale bar=100 μm.

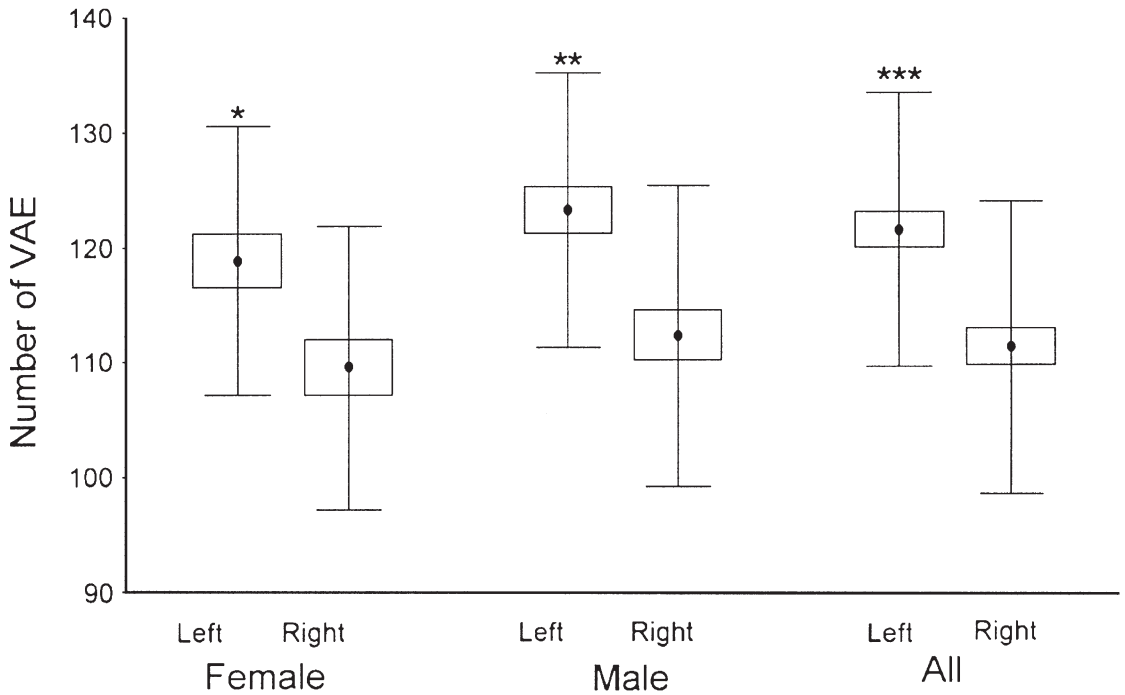

Fig. 4. Hemispheric and gender differences in the number of VAE. The dots represent mean value, the bars represent the S.D., and the boxes, the S.E.M. The number of VAE is higher in the left hemisphere in both women (* $P<0.01$) and men (** $P<0.001$), as well as when all the subjects are taken together (*** $P<0.001$).

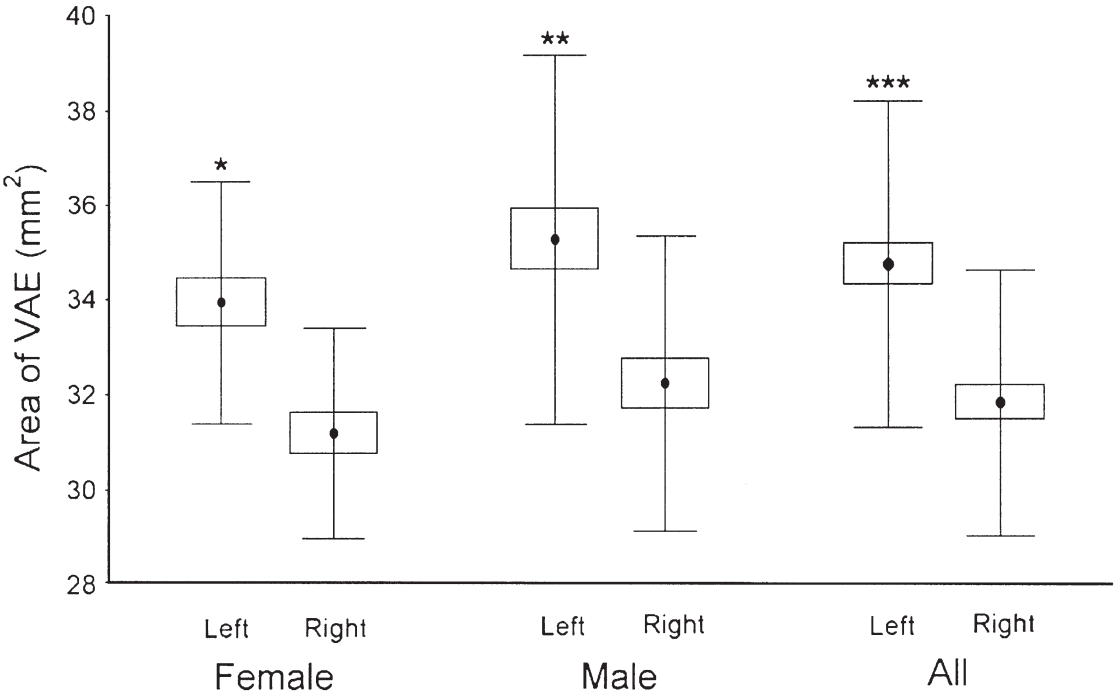

Fig. 5. Hemispheric and gender differences in the area occupied by VAE. The dots represent mean value, the bars represent the S.D., and the boxes, the S.E.M. The VAE area is higher in the left hemisphere in both women (* $P<0.001$) and men (** $P<0.001$), and when all the subjects are analyzed together (*** $P<0.001$).

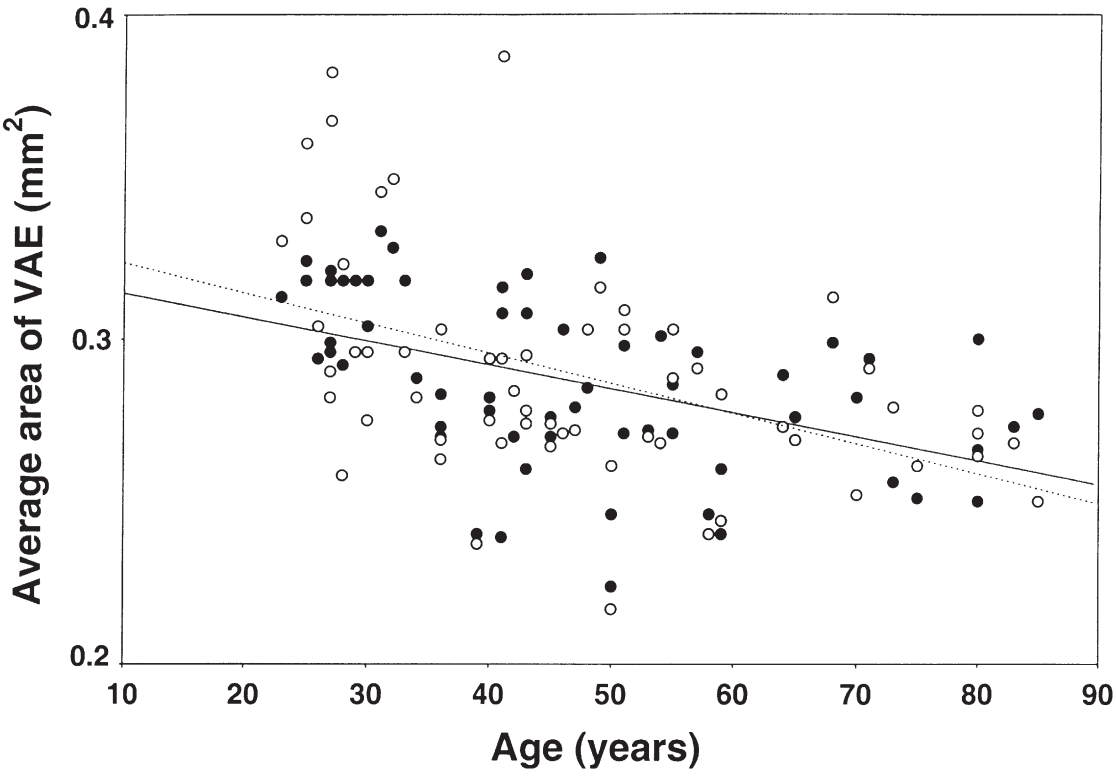

Fig. 6. Average area of single VAE in the left (solid circles, continuous regression line) and the right hemisphere (open circles, dashed regression line), as a function of age.

Table 2. Neuronal number estimates using the optical fractionator method

Case no.	Age (yr.)	Gender	ssf	a_{frame} (μm^2)	a_{step} (10^6 μm)	asf	t (μm)	H (μm)	tsf	Sum Q	N_N left (10^6)	N_N right (10^6)	N_N total (10^6)
15	32	M	0.167	5256	0.96	0.0055	20	10	0.5	289	0.633		
20	36	F	0.167	5256	0.96	0.0055	20	10	0.5	280		0.614	
30	43	F	0.167	5256	0.96	0.0055	20	10	0.5	225	0.493		
31	45	F	0.167	5256	0.96	0.0055	20	10	0.5	291	0.638		
36	49	M	0.167	5256	0.96	0.0055	20	10	0.5	231	0.506		
37	50	M	0.167	5256	0.96	0.0055	20	10	0.5	186/194	0.408	0.425	0.833
49	64	M	0.167	5256	0.96	0.0055	20	10	0.5	197		0.432	
51	68	M	0.167	5256	0.96	0.0055	20	10	0.5	160/155	0.351	0.340	0.691
57	80	M	0.167	5256	0.96	0.0055	20	10	0.5	154		0.338	
59	83	M	0.167	5256	0.96	0.0055	20	10	0.5	112/129	0.245	0.283	0.528

higher in the left than in the right hemisphere, indicating an anatomical asymmetry of the entorhinal cortex. This finding is in a general agreement with the study of Heinsen et al. (1994). By analogy with other brain regions, this suggests that more functionally distinct cortical columns are present in the left entorhinal cortex. However, since the difference in neuron number between hemispheres did not reach statistical significance, it is possible that the left entorhinal cortex is richer in neuronal dendritic arborizations and neuropil volume. The dominance of the left hemisphere in the number and size of VAE is best illustrated by the fact that there were no brains with the same or higher numbers of VAE in the right hemisphere. Only two of 60 brains had comparable VAE area in both hemispheres (all others were larger on the left). On average, the numbers and surface area of VAE, as well as the asymmetry coefficient, were slightly higher in men than in women, but these differences were not significant.

The strongest anatomical asymmetry in the brain is the size of the planum temporale, which is larger on the left side in 69–90% of reported cases, averaging of 78% of the subjects in 22 studies (Shapleske et al., 1999). The present data show that 96.7% of subjects have a larger entorhinal cortex on the left side, potentially making the entorhinal region the most consistently lateralized part of the human brain. Layer II entorhinal neurons receive major inputs from the ipsilateral auditory association areas, such as Brodmann area 22 (in the superior temporal gyrus) that projects mostly to the medial sector of the entorhinal cortex, and Brodmann area 52 (parainsular cortex) that projects mostly to the lateral division of the entorhinal cortex (Amaral et al., 1983; Insausti et al., 1987). Since areas 22 and 52, together with Broca's motor-speech area (Brodmann areas 44 and 45; Amunts et al., 2003), consistently show anatomical and functional leftward asymmetry from early infancy (Karbe et al., 1995; Galuske et al., 2000), it is reasonable to speculate that the larger size of the entorhinal area on the left side may play a role in memory processing of language in the left hemisphere. Because the entorhinal cortex serves as a gateway between the neocortex and the hippocampus, and plays a key role in the processes of memory and learning (Murray and Mishkin, 1986; Zola-Morgan et al., 1989; Fernández et al., 1999; Eichenbaum, 2000), this may also explain the dominance of the left hippocampus (or left medial temporal lobe in general) compared with the right in its capacity for verbal episodic memory (Milner, 1970; Damasio and Geschwind, 1984; Kelley et al., 1998). Based on dissociated verbal and nonverbal retrieval and learning in a subject with circumscribed anterior temporal damage (that included the left entorhinal cortex and hippocampus and the left anterolateral association cortices), a functional asymmetry of the entorhinal cortex with the left (dominant) side being more involved in verbal and the right in non-verbal processing has been proposed (Tranel, 1991). Recent findings obtained using voxel-based mapping of the correlations between cognitive scores and resting state brain glucose utilization measured by positron emission tomography in early AD further support this observation (Eustache et al., 2001). These authors showed that disruption of the left entorhinal cortex causes verbal episodic memory deficit (Eustache et al., 2001). This is also consistent with postmortem data showing that this brain area is affected earliest and most severely by tau pathology in AD (Hirano and Zimmerman, 1962; Hyman et al., 1984; Morrison and Hof, 1997; Giannakopoulos et al., 1998). By using MRI volumetry, decreased memory performance in AD has also been shown to correlate with an increased rate of entorhinal cortex atrophy, with the left side being more affected (Du et al., 2003).

Although we did not observe a significant difference in the number of VAE when comparing near age groups (but only when comparing subjects aged 20–29 years with subjects aged 50–59, 60–69, 70–79 and 80–89 years of age), we found an overall tendency toward a higher number of VAE with aging. As the area of VAE with aging does not follow this trend, it is possible that the higher number of VAE in old individuals results from neuronal loss, so that some VAE became 'split' during aging. It should however be kept in mind that VAE become more clearly visible after fixation, and that the degree and duration of fixation and differential shrinkage may affect the number of VAE present in a given case. A potential source of confound may also lie in differences in the 'clustering' of layer II neurons due to age-related reorganization. Nonetheless, the casting method described in this study offers reliable identification of individual entorhinal islands distribution patterns. This may be a useful and straightforward way to assess interindividual modular variability in the distribution of the neurons of origin of the perforant afferents

Table 3. Comparison with other estimates

	Number of cases studied	Total number of neurons (thousands)		Age-related neuron loss (coefficient of correlation)		Only neurons in entorhinal islands counted	Method/basis for topographical delineation of the entorhinal cortex
		Left	Right	Left	Right		
Present study	10	468	405	−0.91 (7 Subjects from 32 to 83 years of age)	−0.93 (6 Subjects from 36 to 83 years of age)	Yes	Optical fractionator method/VAE
Heinsen et al., 1994	22	92	88	−0.63 (From 18 to 86 years of age)	−0.49 (From 18 to 86 years of age)	Yes	Optical disector method/ clusters of layer II neurons in only those parts of the EC with a lamina dissecans (which is about 25% smaller than area defined on the basis of VAE)
Gómez-Isla et al., 1996	10	650	Not counted	0.0001 (60–89 Years of age)	Not calculated	No (all layer II neurons counted)	Optical disector method/ cytoarchitectonic definition of EC borders that is wider than the EC area with only cell islands. Definition used has about 50% shorter anterior extent of the EC than in the study of West and Slomianka, 1998.
Krimer et al., 1997b	8	2	Not counted	Not calculated	Not calculated	Yes	Optical disector method/ cytoarchitectonic criteria of five sub-areas as defined by Krimer et al., 1997a. Reported neuron numbers counted in only three sub-areas.
West and Slomianka, 1998	5	1100	Not counted	Not calculated	Not calculated	No (all layer II neurons counted)	Optical fractionator method/widest cytoarchitectonic definition of eight sub-areas and their borders, as described in Insausti et al., 1995.
Kordower et al., 2001	8	640	Not counted	64% Neuron loss in 10 old subjects with mild cognitive impairment (80–97 years of age)	Not calculated	No (all layer II neurons counted)	Optical disector method/ widest cytoarchitectonic definition of eight sub-areas and their borders, as described in Insausti et al., 1995.
Hof et al., 2003	17	779	Not counted	30% Loss in old subjects with cognitive impairment	Not calculated	No (all layer II neurons counted)	Optical fractionator method/widest cytoarchitectonic definition of eight sub-areas and their borders, as described in Insausti et al., 1995.

to the dentate gyrus by defining unique patterns of 'individual entorhinal fingerprints.' The fact that these patterns change during aging may have further implications for the study of age-related dementing illnesses such as AD. As a relatively simple method to analyze globally and quantitatively this well-defined population of neurons, it may detect localized pathological changes during aging and AD in a non-invasive manner.

Interestingly, clusters of layer II entorhinal neurons in the superficial portions of layer III (so-called 'heterotopias') have been considered a possible neuroanatomical marker in schizophrenic and depressive patients (Bernstein et al.,

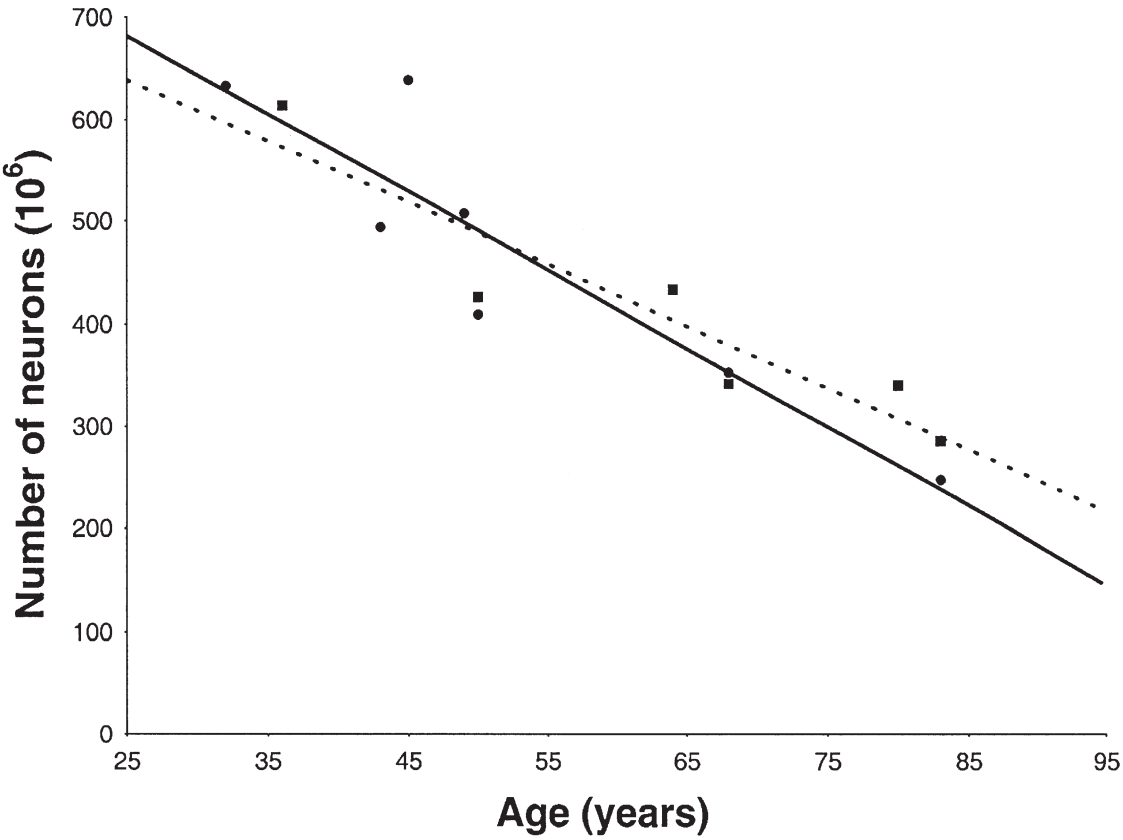

Fig. 7. Age-related changes in numbers of layer II neurons of the entorhinal cortex. Solid circles and the continuous regression line represent the left, and solid squares and the dashed regression line the right hemisphere. Note that there is not much of a cell loss in aging within an old population from about 65 years on, but only when one compares old people with very young cases.

1998). However, our previous observations (Kelovic and Kostovic, 1981; Simic et al., 1995) and the present data clearly indicate that clusters of small neurons with the morphological appearance of late neuroblasts are common in layer II in rostral subfields of the entorhinal cortex in normal young and elderly adults, and thus may not represent a reliable neuroanatomical marker of schizophrenia. The changes observed in the entorhinal cortex in schizophrenia are thus likely to consist of more subtle cellular and molecular disturbances (Akbarian et al., 1993; Hemby et al., 2002). Additional studies will be necessary to clarify this issue.

It should be noted that substantial discrepancies in entorhinal neuron number estimates exist among different studies (Heinsen et al., 1994; Gómez-Isla et al., 1996; Krimer et al., 1997a,b; West and Slomianka, 1998; Kordower et al., 2001; Hof et al., 2003; Bussière et al., 2003). As pointed out by West and Slomianka (1998) and Hof and colleagues (2003), one of the main reasons for this likely lies in the lack of uniform topographical delineation (Table 3). Thus, estimates of neuron numbers obtained by Heinsen et al. (1994) are lower than ours, possibly due to their definition of the entorhinal cortex that included only those parts of the entorhinal cortex where the lamina dissecans is present (which is only a portion of the region defined as entorhinal cortex in our study; Table 3). Other estimates (Gómez-Isla et al., 1996; West and Slomianka, 1998; Kordower et al., 2001; Hof et al., 2003) are higher, probably owing to a more inclusive definition of the entorhinal cortex and the fact that these authors counted all layer II neurons (including neurons in cell bridges among the entorhinal islands), and not just only those strictly located within VAE. As there is no standard nomenclature for the cytoarchitectonic fields included in the entorhinal region, the approach described here using VAE, may be advantageous in the context of comparative studies of disorders of the nervous system such as dementing conditions and schizophrenia. It has been indeed proposed that schizophrenia may be a disorder of the mechanisms that control the development of cerebral asymmetry (Crow, 2000). Besides schizophrenia, atypical patterns of brain organization and hemisphere specialization have also been proposed in developmental dyslexia (Witelson, 1977; Galaburda et al., 1985), autism and Asperger syndrome (Hier et al., 1979; Chiron et al., 1995; Müller et al., 1999), and Williams syndrome (Galaburda and Bellugi, 2000; Reiss et al., 2000).

Layer II entorhinal neurons have been consistently shown to be the first to show age-related neurofibrillary changes (Hirano and Zimmerman, 1962; Hyman et al., 1984; Morrison and Hof, 1997; Giannakopoulos et al., 1998). Heinsen and colleagues (1994) reported negative correlations of the number of layer II neurons with age on both sides, with a mean 26.5% neuron loss in

20–85 year old subjects. Our results obtained by the fractionator method showed comparable, but even greater age-related neuron loss in the entorhinal islands (Table 3), with a 43.5% average neuron loss in 32–83 year old subjects (34% in the left and 51% in the right entorhinal cortex). Moreover, Kordower et al. (2001) recently reported a 64% loss of layer II entorhinal neurons associated with only mild cognitive impairment in 10 subjects aged 80–97 years, which was even more than a 58% neuron loss estimated in their AD group. Conversely, Gómez-Isla et al. (1996) did not observe significant age-related loss of layer II entorhinal neurons in the left hemisphere of 10 normal 60–89 years of age subjects with a Clinical Dementia Rating score of 0. Finally, Hof et al. (2003) showed that a considerable proportion (73–77%) of entorhinal layer II neurons affected by neurofibrillary degeneration might preserve some function even at stages with a Clinical Dementia Rating score of 3. Besides possible differences in small sample size and owing to considerable interindividual variability in entorhinal modules number, size and distribution, an important source of discrepancy among studies arises from the fact that most AD studies have focused on elderly people without considering the possibility of a gradual neuronal loss over adult life prior to the occurrence of AD-related changes. As long as elderly patients do not suffer from AD, they appear neuropathologically quite comparable as a group (Kordower et al., 2001; Hof et al., 2003). It is therefore not surprising that significant neuron loss due solely to aging cannot be revealed without younger adult cases included in the regressions (e.g. Gómez-Isla et al., 1996). On the other hand, when neuronal loss attributable to aging is superimposed to an unbiased estimate of the number of neurofibrillary tangles in AD, regions like the entorhinal cortex and hippocampal formation may display neuronal losses larger than that accounted for by tangle counts alone (Gómez-Isla et al., 1996, 1997; Simic et al., 1998a; Krill et al., 2002). It can be assumed that the pattern of neuron loss does not necessarily match the pattern of tangle formation due to mechanisms other than neurofibrillary degeneration (Simic et al., 1998a, 1998b; Hof et al., 2003).

In conclusion, the relationships between aging and neuron loss in the entorhinal cortex appear to be quite complex. Although the present study indicates that neuron loss is taking place in human entorhinal cortex during normal aging, future quantitative studies based on unbiased stereological principles on larger samples of human brains and strict anatomical criteria are needed to further our understanding of the particular vulnerability of this region.

Acknowledgments—Supported by Croatian Ministry of Science and Technology, grant no. 0108-258 to G.S., and by NIH grants AG02219 and AG05138 (to P.R.H.). The authors thank Zdenka Cmuk, Danica Budinscak and Bozica Popovic for excellent technical assistance.

REFERENCES

Akbarian S, Vinuela A, Kim JJ, Potkin SG, Bunney WE, Jones EG (1993) Distorted distribution of nicotinamide-adenine dinucleotide phosphate-diaphorase neurons in temporal lobe of schizophrenics implies anomalous cortical development. Arch Gen Psychiatry 50:178–187.

Amaral DG, Insausti R, Cowan WM (1983) Evidence for a direct projection from the superior temporal gyrus to the entorhinal cortex in the monkey. Brain Res 275:263–277.

Amunts K, Schleicher A, Bürgel U, Mohlberg H, Uylings HBM, Zilles K (1999) Broca's region revisited: cytoarchitecture and intersubject variability. J Comp Neurol 412:319–341.

Amunts K, Schleicher A, Ditterich A, Zilles K (2003) Broca's region: cytoarchitectonic asymmetry and developmental changes. J Comp Neurol 465:72–89.

Arnold SE, Hyman BT, Hoesen GW, Damasio AR (1991) Some cytoarchitectural abnormalities of the entorhinal cortex in schizophrenia. Arch Gen Psychiatry 48:625–632.

Bernstein HG, Krell D, Baumann B, Danos P, Falkai P, Diekman S, Henning H, Bogerts B (1998) Morphometric studies of the entorhinal cortex in neuropsychiatric patients and controls: clusters of heterotopically displaced lamina II neurons are not indicative of schizophrenia. Schizophr Res 33:125–132.

Bexheti S, Kelovic Z, Kostovic I (1988) "Modular" cytoarchitectonic organization of the human entorhinal cortex. Zürich: European Neuroscience Association Annual Meeting, p. 251.

Bouras C, Hof PR, Morrison JH (1993) Neurofibrillary tangle densities in the hippocampal formation in a non-demented population define subgroups of patients with differential early pathologic changes. Neurosci Lett 153:131–135.

Bouras C, Hof PR, Giannakopoulos P, Michel JP, Morrison JH (1994) Regional distribution of neurofibrillary tangles and senile plaques in the cerebral cortex of elderly patients: a quantitative evaluation of a one-year autopsy population from a geriatric hospital. Cereb Cortex 4:138–150.

Braak H (1972) Zur Pigmentarchitektonik der Grosshirnrinde des Menschen: I. Regio entorhinalis. Z Zellforsch 127:407–438.

Braak H (1980) Architectonics of the human telencephalic cortex, p 37. Berlin: Springer.

Braak H, Braak E (1991) Neuropathological stageing of Alzheimer-related changes. Acta Neuropathol 82:239–259.

Braak H, Braak E (1992) The human entorhinal cortex: normal morphology and lamina-specific pathology in various diseases. Neurosci Res 15:6–21.

Broca P (1861) Perte de la parole: ramollisement chronique et destruction partielle du lobe antérieur gauche du cerveau. Bull Soc Anthropol (Paris) 2: 235–238.

Broca P (1865) Sur la faculté du langage articulé. Bull Soc Anthropol (Paris) 6:493–494.

Brodmann K (1909) Vergleichende Lokalisationslehre der Groβ hirnrinde. Leipzig: Barth.

Bussière T, Gold G, Kövari E, Giannakopoulos P, Bouras C, Perl DP, Morrison JH, Hof PR (2003) Stereologic analysis of neurofibrillary tangle formation in prefrontal cortex area 9 in aging and Alzheimer's disease. Neuroscience 117:577–592.

Chiron C, Leboyer M, Leon F, Jambaque I, Nuttin C, Syrota A (1995) SPECT of the brain in childhood autism: evidence for a lack of normal hemispheric asymmetry. Dev Med Child Neurol 37:849–860.

Crow TJ (2000) Schizophrenia as the price that *Homo sapiens* pays for language: a resolution of the central paradox in the origin of the species. Brain Res Rev 31:118–129.

Damasio AR, Geschwind N (1984) The neural basis of language. Annu Rev Neurosci 7:127–147.

Du AT, Schuff N, Zhu XP, Jagust WJ, Miller BL, Reed BR, Kramer JH, Mungas D, Yaffe K, Chui HC, Weiner MW (2003) Atrophy rates of entorhinal cortex in AD and normal aging. Neurology 60:481–486.

Eichenbaum H (2000) A cortical-hippocampal system for declarative memory. Nat Rev Neurosci 1:41–50.
Eidelberg D, Galaburda AM (1982) Symmetry and asymmetry in the human posterior thalamus: I. Cytoarchitectonic analysis in normal persons. Arch Neurol 39:325–339.
Eidelberg D, Galaburda AM (1984) Inferior parietal lobule: divergent architectonic asymmetries in the human brain. Arch Neurol 41:843–852.
Eustache F, Desgranges B, Giffard B, de la Sayette V, Baron JC (2001) Entorhinal cortex disruption causes memory deficit in early Alzheimer's disease as shown by PET. Neuroreport 12:683–685.
Falkai P, Bogerts B, Rozumek M (1988) Limbic pathology in schizophrenia: the entorhinal region: a morphometric study. Biol Psychiatry 24:515–521.
Falzi G, Perrone P, Vignolo L (1982) Right-left asymmetry in anterior speech region. Arch Neurol 39:239–240.
Fernández G, Brewer JB, Zhao Z, Glover GH, Gabrieli DE (1999) Level of sustained entorhinal activity at study correlates with subsequent cued-recall performance: a fMRI study with high acquisition rate. Hippocampus 9:35–44.
Galaburda AM, Sherman GF, Rosen GD, Aboitiz F, Geschwind N (1985) Developmental dyslexia: four consecutive patients with cortical anomalies. Ann Neurol 18:222–233.
Galaburda AM, Corsiglia J, Rosen GD, Sherman GF (1987) Planum temporale asymmetry, reappraisal since Geschwind and Lewitsky. Neuropsychologia 25:853–868.
Galaburda AM, Bellugi U (2000) Multi-level analysis of cortical neuroanatomy in Williams syndrome. J Cogn Neurosci 12:74–88.
Galuske RA, Schlote W, Bratzke H, Singer W (2000) Interhemispheric asymmetries of the modular structure in the human temporal cortex. Science 289:1946–1949.
Gannon PJ, Holloway RL, Broadfield DC, Braun AR (1998) Asymmetry of chimpanzee planum temporale: humanlike pattern of Wernicke's brain language area homolog. Science 279:220–222.
Geschwind N, Levitsky W (1968) Human brain: left-right asymmetries in temporal speech region. Science 161:186–187.
Giannakopoulos P, Hof PR, Michel J-P, Guimon J, Bouras C (1998) Cerebral cortex pathology in aging and Alzheimer's disease: a quantitative survey of large hospital-based geriatric and psychiatric cohorts. Brain Res Rev 25:217–245.
Gómez-Isla T, Price JL, McKeel DW, Morris JC, Growdon JH, Hyman BT (1996) Profound loss of layer II entorhinal cortex neurons occurs in very mild Alzheimer's disease. J Neurosci 16:4491–4500.
Gómez-Isla T, Hollister R, West H, Mui S, Growdon JH, Petersen JC, Parisi JE, Hyman BT (1997) Neuronal loss correlates with but exceeds neurofibrillary tangles in Alzheimer's disease. Ann Neurol 41:17–24.
Gundersen HJG (1986) Stereology of arbitrary particles: a review of unbiased number and size estimators and the presentation of some new ones. J Microsc 143:3–45.
Hanke J (1997) Sulcal pattern of the anterior parahippocampal gyrus in the human adult. Anat Anzeiger 179:335–339.
Heinsen H, Henn R, Eisenmenger W, Gö tz M, Bohl J, Bethke B, Lockemann U, Püschel K (1994) Quantitative investigations on the human entorhinal area: left-right asymmetry and age-related changes. Anat Embryol 190:181–194.
Heinsen H, Gössmann E, Rüb U, Eisenmenger W, Bauer M, Ulmar G, Bethke B, Schüler M, Schmitt H-P, Götz M, Lockemann U, Püschel K (1996) Variability in the human entorhinal region may confound neuropsychiatric diagnoses. Acta Anat 157:226–237.
Hemby SE, Ginsberg SD, Brunk B, Arnold SE, Trojanowski JQ, Eberwine JH (2002) Gene expression profile for schizophrenia: discrete neuron transcription patterns in the entorhinal cortex. Arch Gen Psychiatry 59:631–640.
Hier DB, Le May M, Rosenberger PB (1979) Autism and unfavorable left-right asymmetries of the brain. J Autism Dev Disord 9:153–159.
Hirano A, Zimmerman HM (1962) Alzheimer's neurofibrillary changes: a topographic study. Arch Neurol 7:227–242.
Hof PR, Bussière T, Gold G, Kövari E, Giannakopoulos P, Bouras C, Perl DP, Morrison JH (2003) Stereologic evidence for persistence of viable neurons in layer II of the entorhinal cortex and the CA1 field in Alzheimer's disease. J Neuropathol Exp Neurol 62:55–67.
Hyman BT, Damasio AR, Van Hoesen GW, Barnes CL (1984) Alzheimer's disease: cell specific pathology isolates the hippocampal formation. Science 225:1168–1170.
Hyman BT, Van Hoesen GW, Kromer LJ, Damasio AR (1986) Perforant pathway changes and the memory impairment of Alzheimer's disease. Ann Neurol 20:472–481.
Insausti R, Amaral DG, Cowan WM (1987) The entorhinal cortex of the monkey: II. Cortical afferents. J Comp Neurol 264:356–395.
Insausti R, Tuñón T, Sobreviela T, Insausti AM, Gonzalo LM (1995) The human entorhinal cortex: a cytoarchitectonic analysis. J Comp Neurol 355:171–198.
Jakob H, Beckmann H (1986) Prenatal developmental disturbances in the limbic allocortex in schizophrenics. J Neural Transm 65:303–326.
Karbe H, Wurker M, Herholz K, Ghaemi M, Pietrzyk U, Kessler J, Heiss WD (1995) Planum temporale and Brodmann's area 22: magnetic resonance imaging and high-resolution positron emission tomography demonstrate functional left-right asymmetry. Arch Neurol 52:869–874.
Kelovic Z, Kostovic I (1981) Banding pattern in human entorhinal cortex revealed by acetylcholinesterase histochemistry. Anat Rec 199:135–136.
Kelovic Z, Bexheti S, Kostovic I (1988) External morphological aspects of the "modular" organization of the human entorhinal area, p 126. Zürich: Anatomische Gesellschaft Versammlung.
Kelley WM, Miezin FM, McDermott KB, Buckner RL, Raichle ME, Cohen NJ, Ollinger JM, Akbudak E, Conturo TE, Snyder AZ, Petersen SE (1998) Hemispheric specialization in human dorsal frontal cortex and medial temporal lobe for verbal and nonverbal memory encoding. Neuron 20:927–936.
Klingler J (1948) Die makroskopische Anatomie der Ammonsformation. Denkschriften der Schweizerischen Naturforschenden Gesellschaft. Zürich: Gebrü der Fretz Ag.
Kordower JH, Chu Y, Stebbins GT, DeKosky ST, Cochran EJ, Bennett D, Mufson EJ (2001) Loss and atrophy of layer II entorhinal cortex neurons in elderly people with mild cognitive impairment. Ann Neurol 49:202–213.
Krill JJ, Patel S, Harding AJ, Halliday GM (2002) Neuron loss from the hippocampus of Alzheimer's disease exceeds extracellular neurofibrillary tangle formation. Acta Neuropathol 103:370–376.
Krimer LS, Hyde TM, Herman MM, Saunders RC (1997a) The entorhinal cortex: an examination of cyto- and myeloarchitectonic organization in humans. Cereb Cortex 7:722–731.
Krimer LS, Herman MM, Saunders RC, Boyd JC, Hyde TM, Carter JM, Kleinman JE, Weinberger DR (1997b) A qualitative and quantitative analysis of the entorhinal cortex in schizophrenia. Cereb Cortex 7:732–739.
Milner B (1970) Memory and the medial temporal regions of the brain. In: Biology of memory (Pribram KH, Broadbent DE, eds), pp 29–70. New York: Academic Press.
Morrison JJ, Hof PR (1997) Life and death of neurons in the aging brain. Science 278:412–419.
Murray EA, Mishkin M (1986) Visual recognition in monkeys following rhinal cortical ablations combined with either amygdalectomy or hippocampectomy. J Neurosci 6:1991–2003.
Müller RA, Behen ME, Rothermel RD, Chugani DC, Muzik O, Mangner TJ, Chugani HT (1999) Brain mapping of language and auditory perception in high-functioning autistic adults: a PET study. J Autism Dev Disord 29:19–31.
Pfeifer RA (1936) Pathologie der Hörstrahlung und der corticalen Hörspähre. In: Handbuch der Neurologie, Vol. 6 (Bumke O, Förster O, eds), pp 523–626. Berlin: Springer.
Rakic P, Nowakowski RS (1981) The time of origin of neurons in the hippocampal region of the rhesus monkey. J Comp Neurol 196:99–128.

Ramón y Cajal S (1901–1902) Sobre un ganglio especial de la corteza esfeno-occipital. Trab Lab Invest Biol Univ Madrid 1:189–206.

Retzius G (1896) Das Menschenhirn Studien in der makroskopischen Morphologie [Table 51, Fig. 5]. Stockholm: Königliche Buchdruckerei P. A. Norstedt & Söner.

Reiss AL, Eliez S, Schmitt JE, Straus E, Lai Z, Jones W, Bellugi U (2000) Neuroanatomy of Williams syndrome: a high resolution MRI study. J Cogn Neurosci 12:65–73.

Shapleske J, Rossell SL, Woodruff PWR, David AS (1999) The planum temporale: a systematic, quantitative review of its structural, functional and clinical significance. Brain Res Rev 29:26–49.

Sherwood CC, Broadfield DC, Holloway RL, Gannon PJ, Hof PR (2003) Variability of Broca's area homologue in African great apes: implications for language evolution. Anat Rec 271:276–285.

Simic G, Radonic E, Folnegovic-Smalc V, Petanjek Z, Judas M, Kostovic I (1995) SMI-32 immunocytochemistry of the hippocampus and entorhinal cortex in schizophrenic patients. Eur J Neurosci Suppl 8:152.

Simic G, Kostovic I, Winblad B, Bogdanovic N (1997) Volume and number of neurons of the human hippocampal formation in normal aging and Alzheimer's disease. J Comp Neurol 379:482–494.

Simic G, Winblad B, Bogdanovic N (1998a) Relationship between hippocampal neurofibrillary degeneration and neuronal loss in aging and Alzheimer's disease. Neurobiol Aging (19 Suppl. 4):239.

Simic G, Gnjidic M, Kostovic I (1998b) Cytoskeletal changes as an alternative view on pathogenesis of Alzheimer's disease. Period Biol 100:165–173.

Simic G, Mrzljak L, Fucic A, Winblad B, Lovric H, Kostovic I (1999) Nucleus subputaminalis (Ayala): the still disregarded magnocellular component of the basal forebrain may be human specific and connected with the cortical speech area. Neuroscience 89:73–89.

Simic G, Lucassen P, Krsnik Z, Kruslin B, Kostovic I, Winblad B, Bogdanovic N (2000) nNOS expression in reactive astrocytes correlates with increased cell death related DNA damage in the hippocampus and entorhinal cortex in Alzheimer's disease. Exp Neurol 165:12–26.

Solodkin A, Van Hoesen GW (1996) Entorhinal cortex modules of the human brain. J Comp Neurol 365:610–627.

Tranel D (1991) Dissociated verbal and nonverbal retrieval and learning following left anterior temporal damage. Brain Cogn 15:187–200.

Van Hoesen GW, Hyman BT, Damasio AR (1991) Entorhinal cortex pathology in Alzheimer's disease. Hippocampus 1:1–8.

von Economo C (1927) Zellaufbau der Grosshirnrinde des Menschen. Berlin: Springer.

von Economo C, Koskinas GN (1925) Cytoarchitektonik der Hirnrinde des erwachsenen Menschen, p 747. Wien: Springer.

West MJ, Slomianka L, Gundersen HJG (1991) Unbiased stereological estimation of the total number of neurons in the subdivisions of the rat hippocampus using the optical fractionator. Anat Rec 231:482–497.

West MJ, Slomianka L (1998) Total number of neurons in the layers of the human entorhinal cortex. Hippocampus 8:69–82.

Witelson SF (1977) Developmental dyslexia: two right hemispheres and none left. Science 195:309–311.

Zola-Morgan S, Squire LR, Amaral DG, Suzuki WA (1989) Lesions of perirhinal and parahippocampal cortex that spare the amygdala and hippocampal formation produce severe memory impairment. J Neurosci 9:4355–4370.

(Accepted 16 September 2004)
(Available online 11 November 2004)